J|A|C|S
ARTICLES
Published on Web 11/06/2007

Analysis of an Unprecedented Mechanism for the Catalytic Hydrosilylation of Carbonyl Compounds

Kristine A. Nolin,[1] Jennifer R. Krumper,[2] Michael D. Pluth, Robert G. Bergman, and F. Dean Toste*

Contribution from the Department of Chemistry, University of California, Berkeley, California 94720

Received June 19, 2007; E-mail: fdtoste@berkeley.edu

Abstract: This work details an in-depth evaluation of an unprecedented mechanism for the hydrosilylation of carbonyl compounds catalyzed by $(PPh_3)_2Re(O)_2I$. The proposed mechanism involves addition of a silane Si−H bond across one of the rhenium−oxo bonds to form siloxyrhenium hydride intermediate **2** that reacts with a carbonyl substrate to generate siloxyrhenium alkoxide **4**, which, in turn, affords the silyl ether product. Compelling evidence for the operation of this pathway includes the following: (a) isolation and structural characterization by X-ray diffraction of siloxyrhenium hydride intermediate **2**, (b) demonstration of the catalytic competence of intermediate **2** in the hydrosilylation reaction, (c) ^1H and $^{31}P\{^1H\}$ NMR and ESI-MS evidence for single-turnover conversion of **2** into **1**, (d) observation of intermediate **2** in the working catalyst system, and (e) kinetic analysis of the catalytic hydrosilylation of carbonyl compounds by **1**.

Despite the extensive application of high-oxidation state metal−oxo complexes in oxidation and atom transfer reactions, such complexes have been largely unexplored in nonoxidative transformations.[3] The resistance of metal−oxo compounds to further oxidation makes them attractive air-, moisture-, and reagent-tolerant catalysts; however, oxidative addition pathways are not readily accessible for the reactions mediated by these complexes. This apparent limitation of metal−oxo complexes presents the opportunity to explore new modes of reactivity. In particular, we were drawn to hydrosilylation, as metal-catalyzed hydrosilylation of carbonyls is an attractive one-step alternative to traditional two-step reduction and alcohol protection sequences. The vast majority of known transition-metal-catalyzed hydrosilylation reactions are thought to proceed *via* one of two mechanisms:[4,5] Chalk−Harrod-type oxidative addition pathways for late metals or σ-bond metathesis-type reactions for early metals. As part of our larger program of exploring new modes of reactivity for high-oxidation-state catalysts,[6] we examined the hydrosilylation of aldehydes and ketones with the bench-stable dioxorhenium(V) catalyst $(PPh_3)_2Re(O)_2I$ (**1**).[7] Reaction scope and yield data were described in a recent communication, along with preliminary evidence that **1** mediates hydrosilylation by a previously unprecedented mechanism involving the addition of silane across a Re═O double bond (Scheme 1).[8]

Scheme 1. Proposed Catalytic Cycle

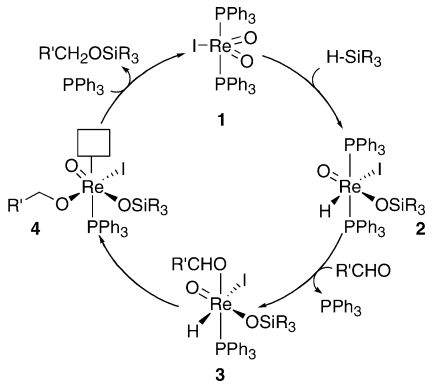

Since our initial report, a number of metal−oxo catalyzed hydrosilylation reactions have been described.[9] Abu-Omar and co-workers recently detailed the catalytic hydrosilylation of carbonyl compounds by the oxorhenium(V) complex $[Re(O)(hoz)_2][TFPB]$ (hoz = 2-(2′-hydroxyphenyl)-2-oxazoline, TFPB = tetrakis(pentafluorophenyl)borate). The authors provide evidence that $[Re(O)(hoz)_2][TFPB]$ acts *via* a σ-bond metathesis

(1) Present location: Department of Chemistry, Harvard University, Cambridge, MA 02138.
(2) Present location: Department of Chemistry, University of California, Irvine, CA 92697-2025.
(3) For several examples, see: (a) *Handbook of Reagents for Organic Synthesis: Oxidizing and Reducing Agents*; Burke, S. D., Danheiser, R. L., Eds.; John Wiley & Sons: New York, 1999. (b) *Comprehensive Organic Synthesis*; Trost, B. M., Fleming, I., Eds.; Pergamon Press: New York, 1991; Vol. 7. (c) Nugent, W. A.; Mayer, J. M. *Metal-Ligand Multiple Bonds*; Wiley: New York, 1988.
(4) (a) Chalk, A. J.; Harrod, J. F. *J. Am. Chem. Soc.* **1965**, *87*, 16. (b) Ojima, I.; Li, Z.; Zhu, J. In *The Chemistry of Organic Silicon Compounds*; Rappoport, Z., Apeloig, Y., Eds.; John Wiley & Sons: New York, 1998; Vol. 2.
(5) (a) Glaser, P. B.; Tilley, T. D. *J. Am. Chem. Soc.* **2003**, *125*, 13640. (b) Parks, D. J.; Blackwell, J. M.; Piers, W. E. *J. Org. Chem.* **2000**, *65*, 3090.
(6) (a) Blanc, A.; Toste, F. D. *Angew. Chem., Int. Ed.* **2006**, *45*, 2096. (b) Nolin, K. A.; Ahn, R. W.; Toste, F. D. *J. Am. Chem. Soc.* **2005**, *127*, 17168. (c) Ohri, R. V.; Radosevich, A. T.; Hrovat, K. J.; Musich, C.; Huang, D.; Holman, T. R.; Toste, F. D. *Org. Lett.* **2005**, *7* (12), 2501. (d) Radosevich, A. T.; Musich, C.; Toste, F. D. *J. Am. Chem. Soc.* **2005**, *127*, 1090. (e) Kennedy-Smith, J. J.; Young, L. A.; Toste, F. D. *Org. Lett.* **2004**, *6* (8), 1325. (f) Sherry, B. D.; Loy, R. N.; Toste, F. D. *J. Am. Chem. Soc.* **2004**, *126*, 4510. (g) Luzung, M. R.; Toste, F. D. *J. Am. Chem. Soc.* **2003**, *125*, 15760. (h) Sherry, B. D.; Radosevich, A. T.; Toste, F. D. *J. Am. Chem. Soc.* **2003**, *125*, 6076.

10.1021/ja074477n CCC: $37.00 **© 2007 American Chemical Society**

Table 1. Reduction of Aldehydes and Ketones

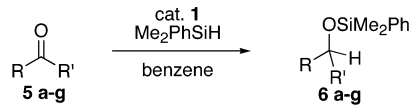

5 a-g **6 a-g**

Entry	Silyl Ether		temp.(°C) / time	yield
1	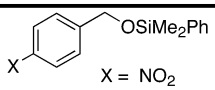 X = NO_2	**6a**	60 / 15 min	94%[a]
2	X = C(O)Me	**6b**	rt / 26 h	86 %[a]
3	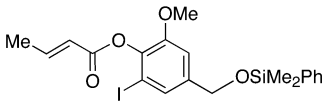	**6c**	60 / 2 h	68%[a]
4	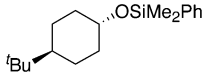	**6d**	75 / 7 h	87%[b,c]
5	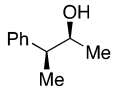	**6e**	rt / 24 h	83%[d,e]
6	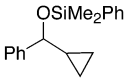	**6f**	75 / 20 h	69%[b]
7	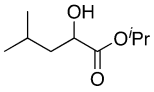	**6g**	rt / 48 h	78%[b,d]

[a] 1.2 equiv silane, 2 mol% **1**, and 0.5 M in benzene. [b] 2 equiv of silane and 5 mol% **1**. [c] >25:1 *trans:cis*. [d] Alcohol isolated after TBAF deprotection. [e] 2 equiv of silane, 5 mol% **1**, and 0.5 M in CH_2Cl_2; 1.5:1 *cis:trans*.

mechanism.[10] A recent computational study by Lin, Wu, and co-workers suggests that similar reactivity is not probable for dioxorhenium(V) hydrosilylation catalyst **1** and that the mechanism we described for these processes was more likely.[11] The mechanistic studies described in this article provide compelling support for the operation of the catalytic mechanism illustrated in Scheme 1 for dioxorhenium catalyst **1**. Our observations include the following: (a) isolation and structural characterization by X-ray diffraction of siloxyrhenium hydride intermediate **2**, (b) demonstration of the catalytic competence of intermediate **2** in the hydrosilylation reaction, (c) ^{1}H and ^{31}P-{^{1}H} NMR and ESI-MS evidence for single-turnover conversion of **2** into **1**, (d) observation of intermediate **2** in the working catalyst system, and (e) kinetic analysis of the formation of **2** from **1** and the catalytic hydrosilylation of carbonyl compounds by **1**.

Results and Discussion

Reduction of Carbonyl Compounds. Dioxorhenium complex **1** was shown to be a highly chemoselective catalyst for the reduction of carbonyl compounds by silanes. The hydrosilylation reaction was readily applied to a variety of aromatic and aliphatic aldehydes and ketones with excellent yields (Table 1). During initial investigations, benzene was used as the solvent; however, CH_2Cl_2, THF, $CHCl_3$, dioxane, toluene, acetonitrile, and ethyl acetate also proved to be suitable solvents at room temperature or elevated temperatures. The mild conditions under which catalyst **1** operates are compatible with a number of sensitive functional groups, including nitro groups, nitriles, olefins, esters, and aryl iodides. The catalyst can also be used for chemoselective reductions of bifunctional molecules. For example, aldehyde **5b** was reduced at room temperature with no reduction of the ketone moiety (Table 1, entry 2). Ketones can also be hydrosilylated by catalyst **1** (entries 4−7). In these systems, however, slightly higher catalyst loading (5 mol % **1**), 2 equiv of silane, and longer reaction times were required. The prolonged reaction times resulted in similar conversions but lower product yields due to hydrolysis of the silyl ether product. The chemoselectivity of catalyst **1** was further demonstrated in the synthesis of α-hydroxyesters by hydrosilylation and subsequent deprotection of the corresponding ketone (Table 1, entry 7). These reduction reactions were catalyzed readily at room temperature with 2 equiv of Me_2PhSiH and 5 mol % **1** with no reduction of the ester functionality.[12] The stereoselectivity of the reduction reaction was examined for the hydrosilylation of 4-*tert*-butylcyclohexanone (Table 1, entry 4) and 3-phenyl-2-butanone (Table 1, entry 5). The hydrosilylation of 4-*tert*-butylcyclohexanone was performed in benzene at 75 °C,

(7) Ciani, G. F.; D'Alfonso, G.; Romiti, P. F.; Sironi, A.; Freni, M. *Inorg. Chem. Acta* **1983**, *72*, 29.
(8) Kennedy-Smith, J. J.; Nolin, K. A.; Gunterman, H. P.; Toste, F. D. *J. Am. Chem. Soc.* **2003**, *125*, 4056.
(9) (a) Royo, B.; Romao, C. C. *J. Mol. Catal. A: Chem.* **2005**, *236*, 107. (b) Reis, P. M.; Romao, C. C.; Royo, B. *Dalton Trans.* **2006**, 1842. (c) Ison, E. A.; Cessarich, J. E.; Du, G. D.; Fanwick, P. E.; Abu-Omar, M. M. *Inorg. Chem.* **2006**, *45*, 2385. (d) Fernandes, A. C.; Romao, C. C. *Tetrahedron Lett.* **2005**, *46*, 8881.
(10) (a) Ison, E. A.; Trivedi, E. R.; Corbin, R. A.; Abu-Omar, M. M. *J. Am. Chem. Soc.* **2005**, *127*, 15374. (b) Du, G. D.; Fanwick, P. E.; Abu-Omar, M. M. *J. Am. Chem. Soc.* **2007**, *129*, 5180.
(11) Chung, L. W.; Lee, H. G.; Lin, Z.; Wu, Y.-D. *J. Org. Chem.* **2006**, *71*, 6000.
(12) Ester reduction observed with MoO_2Cl_2: Fernandas, A. C.; Romao, C. C. *J. Mol. Catal. A: Chem.* **2006**, *253*, 96.

and the silyl ether product was determined to be predominantly in the *trans* (>25:1) configuration. The selectivity for the *trans* product suggests axial delivery of the hydride to the substituted cyclohexanone. The reduction of 3-phenyl-2-butanone was carried out in CH_2Cl_2 at room temperature, and deprotection of the resulting silyl ether by TBAF afforded the alcohol in 83% isolated yield. The reaction proceeds with modest diastereoselectivity and favors the anti-Felkin−Ahn product in a ratio of 1.5:1.[13]

Proposed Catalytic Cycle. We propose that the catalytic cycle for hydrosilylation of carbonyl compounds by **1** begins with the formation of $(PPh_3)_2Re(O)(I)(H)(OSiR_3)$ (**2**, Scheme 1). Complexation of the aldehyde or ketone is preceded by dissociation of one phosphine ligand from **2** and affords siloxyrhenium hydride complex **3**. Subsequent insertion of the datively bound carbonyl substrate of **3** into the Re−H bond yields siloxyrhenium alkoxide complex **4**. Dioxorhenium complex **1** is regenerated by reassociation of phosphine and liberation of the silyl ether product via a formal retro-[2 + 2] reaction between the alkoxy and siloxy ligands of **4**. The experimental results reported here support this proposed mechanism.

Isolation and Characterization of 2a and 2b. To provide direct evidence for the formation of siloxyrhenium hydride intermediates in the catalytic system, we isolated complexes **2a** and **2b** by treating dioxorhenium **1** with monohydridic silanes in the absence of carbonyl-based hydrosilylation substrates (eq 1). A concentrated benzene solution of **1** was treated with

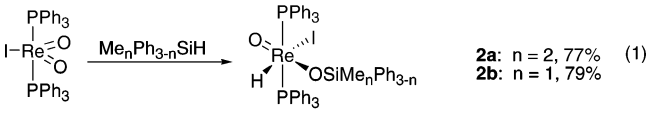

1

Me_2PhSiH (6 equiv) resulting in the precipitation of siloxyrhenium hydride complex **2a** as a tan solid (77%). Complex **2a** was identified by characteristic resonances in its ^1H NMR spectrum at 6.49 ppm (t, 1H, Re−*H*) and −0.77 ppm (s, 6H, Re−OSiPh(CH_3)$_2$).[14] The assignment of the downfield ^1H NMR resonance corresponding to the rhenium-bound hydride ligand was confirmed by synthesis of rhenium deuteride complex *d*-**2a**, which showed no peak at 6.49 ppm in the ^1H NMR spectrum but a resonance at that chemical shift in the ^2H spectrum.[15] Additionally, an IR stretch at 1978 cm^{-1}, assigned to the rhenium−hydride ligand in **2a**, was replaced by a new stretch at 1451 cm^{-1} in *d*-**2a** (predicted = 1399 cm^{-1}). The $^{29}Si\{^1H\}$ spectrum of **2a** (7.5 ppm, s) is consistent with the assignment of the complex as a siloxy, rather than silyl, species.

Although dimethylphenylsiloxyrhenium hydride complex **2a** was consistently formed as a polycrystalline solid, diphenylmethylsiloxyrhenium hydride complex **2b** was isolated as X-ray quality crystals. Treatment of **1** with Ph_2MeSiH afforded the diphenylmethylsiloxyrhenium hydride complex **2b** as a pale gray solid (79%). Spectroscopic characterization of **2b** gave results similar to those observed for **2a**. Grey-green platelike crystals were obtained by slow cooling of a concentrated CH_2Cl_2 solution of **2b** to −30 °C. Although scattered reports indicate that similar reactions are known,[16] the isolation of complexes **2a** and **2b** represents the first reported preparation of siloxymetal hydride[17] complexes by addition of silanes to metal−oxygen double bonds.

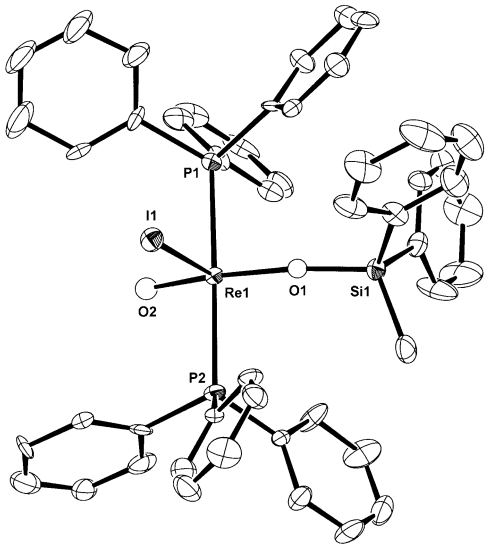

Figure 1. ORTEP drawing of **2b**. Thermal ellipsoids are shown at the 50% probability level. H-atoms have been removed for clarity. Representative bond lengths (Å) and angles (deg): Re(1)−O(1), 1.925(6); Re(1)−O(2), 1.718(6); Re(1)−P(1), 2.505(3); Re(1)−P(2), 2.496(3); P(1)−Re(1)−P(2), 174.1(1); O(1)−Re(1)−O(2), 171.8(4); Re(1)−O(1)−Si(1), 160.5(5).

An ORTEP diagram of the structure of **2b** is presented in Figure 1, along with representative bond lengths and angles. The complex was found to possess octahedral coordination geometry. The triphenylphosphine ligands of **2b** assume a *trans* orientation, as do the oxo and siloxy groups. The rhenium-bound hydride ligand was not located in the electronic difference map, although its position is assumed to be *trans* to the iodine group. The Re−O bond distance for the oxo group is 1.718(6) Å, indicating some triple-bond character.[18] The Re−P bond distances of 2.505(3) and 2.496(3) in **2b** are typical for Re(V)−oxo complexes.[19]

Formation of 2a and 2b. The formation of siloxyrhenium hydride complexes **2a** and **2b** (and, more generally, **2** in the catalytic system) may result from concerted [2 + 2] addition of silane across one Re=O bond (Scheme 2, Path a).[11] An

(13) (a) Yamamoto, Y.; Maruyama, K. *J. Am. Chem. Soc.* **1985**, *107*, 6411. (b) Yamamoto, Y.; Matsuoka, K.; Nemoto, H. *J. Am. Chem. Soc.* **1988**, *110*, 4475.

(14) (a) Paulo, A.; Domingos, A.; Garcia, R.; Santos, I. *Inorg. Chem.* **2000**, *39*, 5669. (b) Reddy, K. R.; Domingos, A.; Paulo, A.; Santos, I. *Inorg. Chem.* **1999**, *38*, 4278.

(15) Wolczanski and coworkers have observed similar downfield chemical shifts for siloxytungsten hydride, siloxytantalum hydride, and silylamidotungsten hydride complexes. (a) Holmes, S. M.; Schafer, D. F., II; Wolczanski, P. T.; Lobkovsky, E. M. *J. Am. Chem. Soc.* **2001**, *122*, 10571. (b) Miller, R. L.; Lawler, K. A.; Bennet, J. L.; Wolczanski, P. T. *Inorg. Chem.* **1996**, *35*, 3242. (c) Miller, R. L.; Toreki, R.; LaPointe, R. E.; Wolczanski, P. T.; Van, Duyne, G. D.; Roe, D. C. *J. Am. Chem. Soc.* **1993**, *115*, 5570. (d) Strazisar, S. A.; Wolczanski, P. T. *J. Am. Chem. Soc.* **2001**, *123*, 4728. (e)LaPointe, R. E.; Wolczanski, P. T. *J. Am. Chem. Soc.* **1986**, *108*, 3535.

(16) (a) Gountchev, T. I.; Tilley, T. D. *J. Am. Chem. Soc.* **1997**, *119*, 12831. (b) Sweeney, Z. K.; Polse, J. L.; Andersen, R. A.; Bergman, R. G.; Kubinec, M. G. *J. Am. Chem. Soc.* **1997**, *119*, 4543. (c) Sweeney, Z. K.; Polse, J. L.; Bergman, R. G.; Andersen, R. A. *Organometallics* **1999**, *18*, 5502.

(17) Miller, R. L.; Lawler, K. A.; Bennet, J. L.; Wolczanski, P. T. *Inorg. Chem.* **1996**, *35*, 3242 and references therein.

(18) (a) Baril-Robert, F.; Beauchamp, A. L. *Can. J. Chem.* **2003**, *81*, 1326. (b) Kremer, C.; Rivero, M.; Kremer, E.; Suescun, L.; Mombrú, A. W.; Mariezcurrena, R.; Domínguez, S.; Mederos, A.; Midollini, S.; Castiñeiras, A. *Inorg. Chim. Acta* **1999**, *294*, 47. (c) Mayer, J. M. *Inorg. Chem.* **1988**, *27*, 3899. (d) Mayer, J. M. *Metal-Ligand Multiple Bonds*; Wiley: New York, 1988. (e) Suescun, L.; Mombrú, A. W.; Mariezcurrena, R. A.; Pardo, H.; Russi, S.; Kremer, C.; Rivero, M.; Kremer, E. *Acta Crystallogr.* **2000**, *56*, 930.

(19) Battistuzzi, R.; Saladini, M. *Inorg. Chim. Acta* **2000**, *304*, 114.

Scheme 2. Formation of Siloxyrhenium Hydride

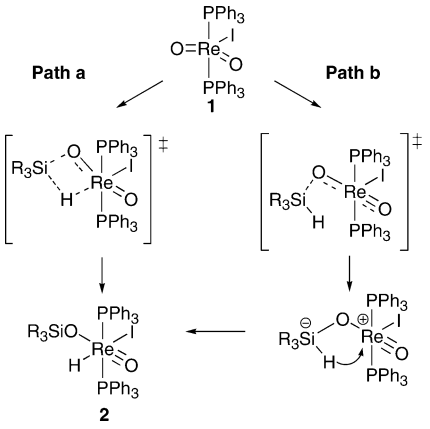

alternative mechanism for silane addition is illustrated as Path b in Scheme 2. Many metal−oxo complexes react as Lewis bases;[20] as such, activation of the Lewis acidic silicon atom by the rhenium-bound oxo ligand could afford a Si^-/Re^+ zwitterion. The silicate group in this intermediate could then deliver the hydride to the metal center, forming complex **2**.[21]

Kinetic analysis of the formation of siloxyrhenium hydride **2a** from **1** and excess (>10 equiv relative to **1**) Me_2PhSiH and **2b** from **1** and excess (>10 equiv relative to **1**) Ph_2MeSiH was conducted. The linear, pseudo-first-order relationship of $\ln([\mathbf{1}]_o/[\mathbf{1}]_o - [\mathbf{2}]_t)$ with time suggests the reaction rate exhibits a first-order dependence on the concentration of **1** (Figures 2A and 3A). The rates of formation of the siloxyrhenium hydrides **2a** and **2b** were found to be independent of the concentration of PPh_3 (Figures 2B and 3B) while exhibiting first-order dependence on the concentration of silane (Figures 2C and 3C). A rate law for the formation of the **2** from **1** and silane that accounts for the above results is given in eq 2. The second-order rate constants were determined from the plots of k_{obs} as a function of the concentration of silane (Figures 2C and 3C) and found to be 6.9×10^{-3} $M^{-1}\cdot s^{-1}$ for the reaction with Me_2PhSiH and 2.3×10^{-3} $M^{-1}\cdot s^{-1}$ for the reaction with Ph_2MeSiH.

$$\text{rate} = k[\text{silane}][\mathbf{1}] = k_{obs}[\mathbf{1}]$$
$$k_{obs} = k[\text{silane}] \qquad (2)$$

The lack of dependence on the concentration of PPh_3 is consistent with a nondissociative mechanism. This is contrary to the computational reports published by Lin, Wu, and coworkers.[11] In their examination of siloxyrhenium hydride formation, these authors predicted that the dissociation of a phosphine ligand prior to silane activation would be more favorable *for the concerted [2 + 2]-addition pathway*. However, the stepwise mechanism for activation of silane by coordination of the Lewis basic oxo ligand followed by hydride transfer (Scheme 2, Path b) was not examined in this computational paper.

An isotope effect was determined for the formation of **2a** and *d*-**2a**. The reactions of **1** with Me_2PhSiH and **1** and Me_2PhSiD were monitored by ^1H NMR spectroscopy at 298 K at the following concentrations: $[\mathbf{1}] = 2.2 \times 10^{-2}$ M and $[Me_2PhSiH] = 2.2 \times 10^{-1}$ M or $[Me_2PhSiD] = 2.2 \times 10^{-1}$ M. Under these conditions, k_{obs} values of $(1.07 \pm 0.02) \times 10^{-3}$ s^{-1} and $(1.46 \pm 0.01) \times 10^{-3}$ s^{-1} were measured for the reactions of Me_2PhSiH and Me_2PhSiD, respectively, giving a k_H/k_D of 0.73 ± 0.02. This inverse secondary isotope effect observed is most consistent with the mechanism illustrated in Path b of Scheme 2: rate-determining formation of a Si^-/Re^+ zwitterion occurs prior to hydride transfer. The lack of a primary isotope effect for this reaction suggests that concerted [2 + 2] addition of silane across the rhenium−oxo bond (Scheme 2, Path a) is not operable in the formation of **2** from **1** and silane.

The presence of a "spectator" oxo ligand, one not involved in the reaction, has been predicted to provide a thermodynamic driving force for addition of reagents across metal−oxo bonds in metathesis and oxidation reactions.[22] The spectator oxo ligand donates π-electron density, stabilizing the intermediates generated by addition across the other metal−oxo bond. Furthermore, reduction of the second oxo ligand relieves competition between the oxo ligands for π-donation to the metal center.[23] For these reasons, we propose that the presence of a second oxo ligand on the rhenium center increases the stability of the siloxyrhenium hydride intermediate **2**.

Catalytic Activity of 2a and 2b. The catalytic activity of the isolated siloxyrhenium hydride complex **2a** was probed in the hydrosilylation of *p*-anisaldehyde with Me_2PhSiH. Side-by-side hydrosilylation reactions using 2 mol % **2a** and **1**, respectively, as catalysts both afforded **7a** in excellent yields (eq 3; catalyst = **1**, 91%; catalyst = **2a**, 92%). The rates for

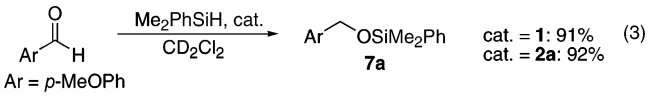

these side-by-side reactions were qualitatively indistinguishable (both gave complete conversion after 1 h at 318 K in CD_2Cl_2) and quantitatively identical ($t_{1/2}$ (40 °C) = 6.7 ± 0.3 min for **1**; $t_{1/2}$ (40 °C) = 6.5 ± 0.3 min for **2a**).

Stoichiometric Hydrosilylation with 2a and 2b. Strong evidence for the intermediacy of siloxyrhenium hydride complexes **2** in the catalytic hydrosilylation of carbonyl compounds by **1** was obtained by stoichiometric single-turnover experiments using complexes **2a** and **2b**. Complexes **2a** and **2b** each react cleanly and rapidly with *p*-anisaldehyde at 318 K *in the absence of added silane* to afford the corresponding hydrosilylated products **7a** and **7b** (eq 4). Importantly, $^{31}P\{^1H\}$ NMR

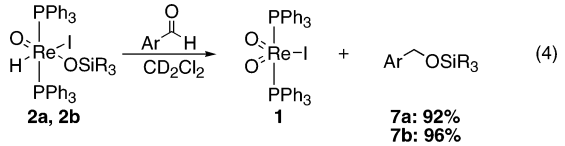

spectroscopy reveals that each of these stoichiometric reactions yields dioxorhenium complex **1** as the primary inorganic

(20) (a) Schatte, G.; Chivers, T.; Tuononen, H. M.; Suontamo, R.; Laitinen, R.; Valkonen, J. *Inorg. Chem.* **2005**, *44*, 443. (b) Fischer, J.; Kress, J.; Osborn, J. A.; Richard, L.; Wesolek *Polyhedron* **1987**, *6*, 1839. (c) Feher, F. J.; Blanski, R. L. *Organometallics* **1993**, *12*, 958. (d) Barrado, G.; Doerrer, L.; Green, M. L. H.; Leech, M. A. *J. Chem. Soc., Dalton Trans.* **1999**, 1061.

(21) Corriu, R. J. P.; Guerin, C.; Henner, B.; Wang, Q. *Organometallics* **1991**, *10*, 2297.

(22) (a) Rappe, A. K.; Goddard, W. A. *J. Am. Chem. Soc.* **1982**, *104*, 448. (b) Rappe, A. K.; Goddard, W. A. *J. Am. Chem. Soc.* **1982**, *104*, 3287.

(23) For additional discussion on the metal−oxo bonding in Re−oxo complexes, see: Lin, Z.; Hall, M. B. *Coord. Chem. Rev.* **1993**, *123*, 149.

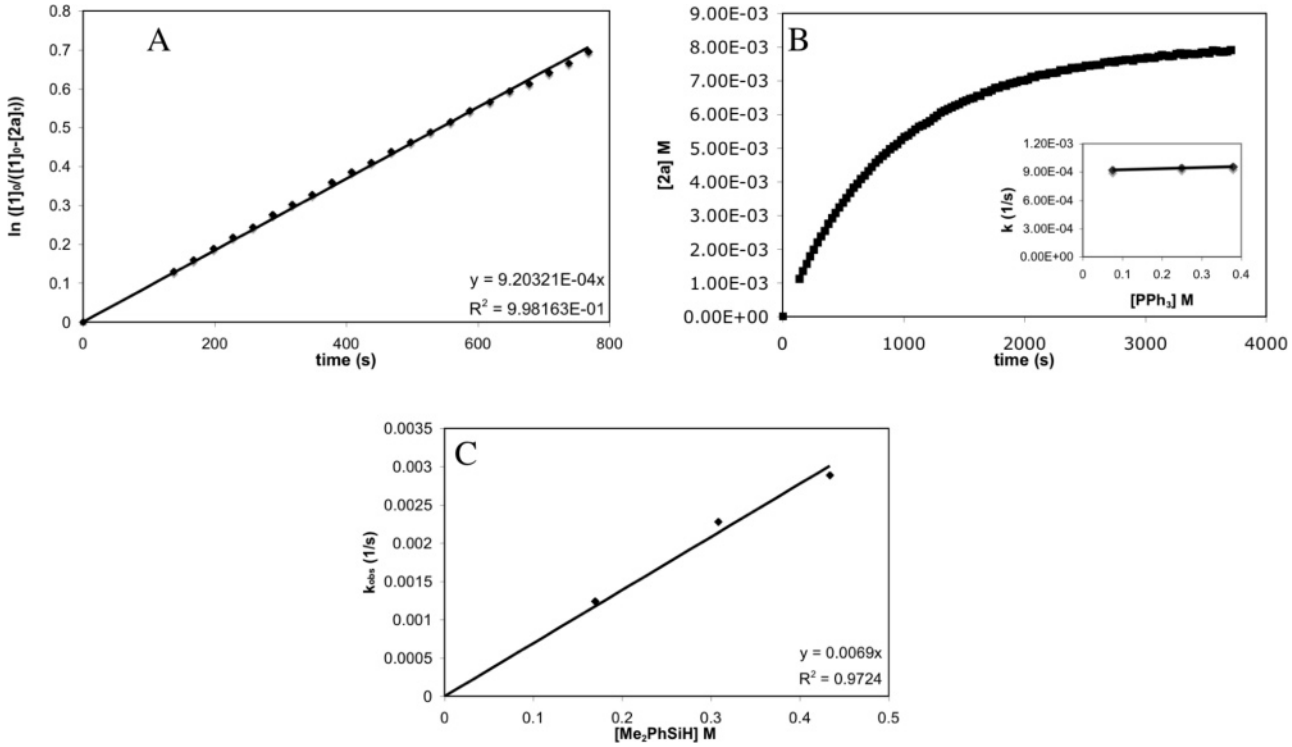

Figure 2. (A) Representative plot of the change in [**2a**] with time for the reaction of **1** with Me_2PhSiH at the following concentrations: [**1**] = 1.3×10^{-2} M, [Me_2PhSiH] = 1.6×10^{-1} M, and [PPh_3] = 7.5×10^{-2} M. The appearance of the Re−OSi*Me*$_2$Ph signal at −0.77 ppm was monitored by ^{1}H NMR spectroscopy at 298 K in CD_2Cl_2. Inset: Relationship of [PPh_3] and k_{obs} at [PPh_3] = 7.5×10^{-2} to 3.8×10^{-1} M. (B) k_{obs} values were determined by plotting the change of $\ln([\mathbf{1}]_0/([\mathbf{1}]_0 - [\mathbf{2a}]))$ with time. The plot shown corresponds to the reaction of **1** with Me_2PhSiH at the following concentrations: [**1**] = 1.3×10^{-2} M, [Me_2PhSiH] = 1.6×10^{-1} M, and [PPh_3] = 7.5×10^{-2} M. (C) Relationship of [Me_2PhSiH] and k_{obs} at [Me_2PhSiH] = 1.7×10^{-1} to 4.3×10^{-1} M, [PPh_3] = 1.1×10^{-1} M, and [**1**] = 1.7×10^{-2} M.

product. The observation of facile stoichiometric silyl group transfer from **2a, b** to a carbonyl substrate strongly supports the feasibility of the Scheme 1 mechanism under working catalytic conditions.

The stoichiometric hydrosilylation of anisaldehyde by **2a** was also monitored by ESI-MS.[24] The positive-mode ESI-MS of a CH_2Cl_2/CH_3CN solution of isolated rhenium hydride **2a** contains a single peak at 879.5 *m*/*z* [**2a** − I]$^+$. The positive-mode ESI-MS spectrum acquired 10 min after mixing **2a** (1.0 mL, 1.24×10^{-2} M in CH_2Cl_2) with anisaldehyde (8.0×10^{-2} mmol) indicates formation of dioxorhenium complex **1** as a peak at 743.3 *m*/*z* [**1** − I]$^+$. The identity of this peak was confirmed in an independently obtained ESI-MS spectrum of isolated dioxorhenium compound **1**. After 45 min at room temperature, **1** was observed to be the major rhenium-containing species in the stoichiometric hydrosilylation reaction solution. These observations mirror results obtained by $^{31}P\{^1H\}$ NMR spectroscopy (see above): in both cases, transfer of the silicon and the hydride groups of **2a** and **2b** to a *p*-anisaldehyde cleanly affords **1**.

Stereoselectivity of Stoichiometric Hydrosilylation with 2a. The stereoselectivity of the reduction of 3-phenyl-2-butanone with **2a** was examined. The reaction was performed in CH_2Cl_2 at 40 °C,[25] and the resultant silyl ether was deprotected by TBAF affording the corresponding alcohol. The reaction proceeds with slight diastereoselectivity and favors the anti-Felkin−Ahn product in a ratio of 1.13:1.[13] This result mirrors that of the analogous reaction with **1** and Me_2PhSiH that also favored the anti-Felkin−Ahn product in a ratio of 1.17:1 (eq 5).

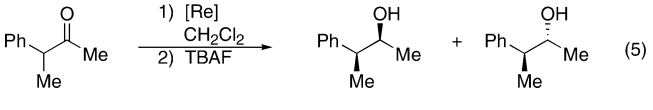

(5)

[Re]			
1 and Me_2PhSiH	1.17	:	1
2a	1.13	:	1

Kinetics of Stoichiometric Hydrosilylation with 2b. Kinetic parameters were determined for the stoichiometric hydrosilylation of *p*-anisaldehyde by **2b** (eq 6). Experiments were

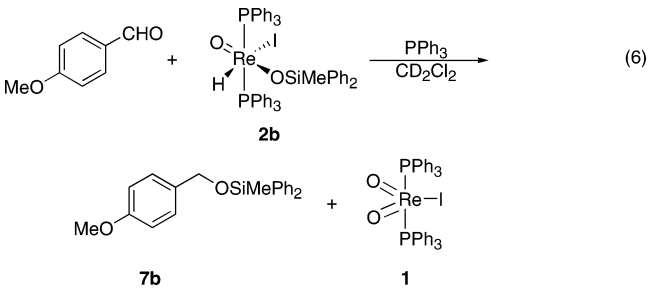

(6)

conducted at 313 K in CD_2Cl_2 in the *absence of silane*. In preliminary studies, small quantities of free triphenylphosphine were observed by $^{31}P\{^1H\}$ NMR spectroscopy in these reactions.

(24) Spectra included in Supporting Information.
(25) At room temperature, **2a** was not completely soluble under the reaction conditions and competitive degradation of **2a** to form **1** and silanol byproducts was observed. A proposed mechanism of this transformation is discussed in a later section.

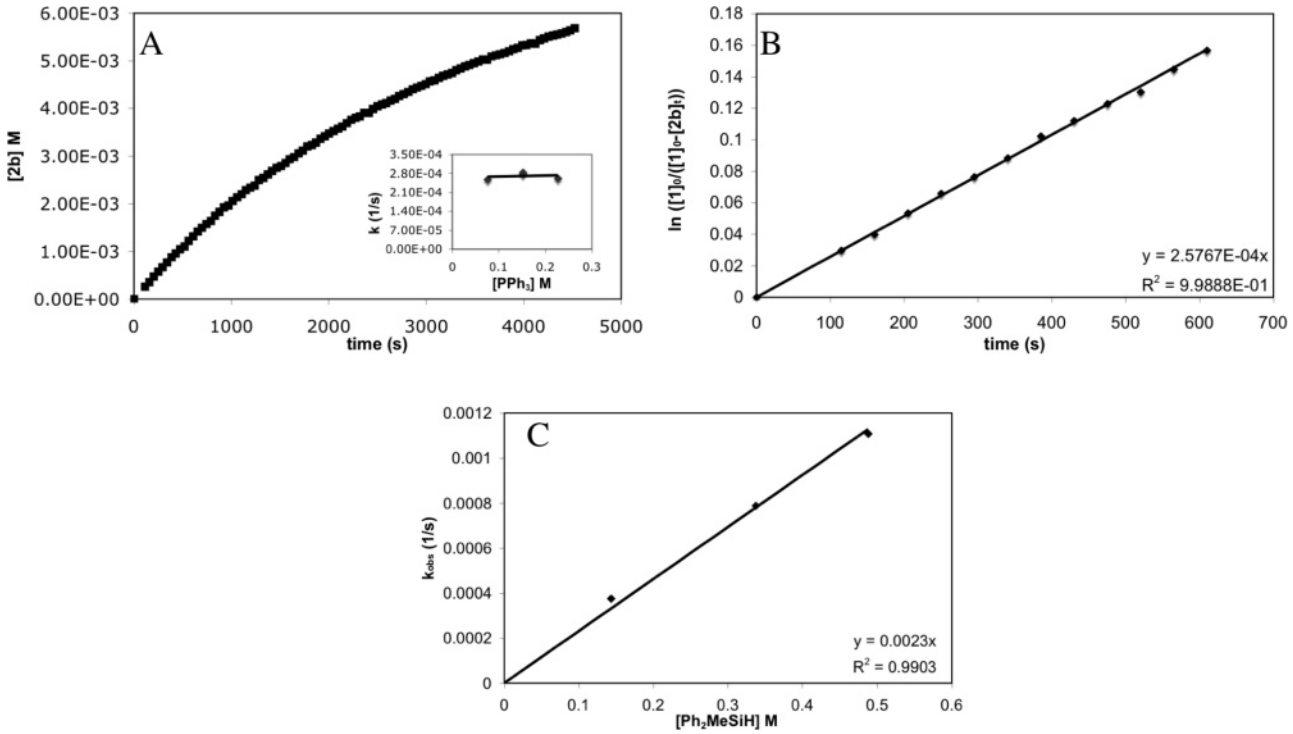

Figure 3. (A) Representative plot of the change in [**2b**] with time for the reaction of **1** with Ph_2MeSiH at the following concentrations: [**1**] = 1.3×10^{-2} M, [Ph_2MeSiH] = 1.6×10^{-1} M, and [PPh_3] = 7.6×10^{-2} M. The appearance of the Re−OSi*Me*Ph_2 signal at −0.66 ppm was monitored by ^1H NMR spectroscopy at 298 K in CD_2Cl_2. Inset: Relationship of [PPh_3] and k_{obs} to [PPh_3] = 7.6×10^{-2} to 2.3×10^{-1} M. (B) K_{obs} were determined by plotting the change of $\ln([\mathbf{1}]_0/([\mathbf{1}]_0 - [\mathbf{2b}]))$ with time. The plot shown corresponds for the reaction of **1** with Ph_2MeSiH at the following concentrations: at [**1**] = 1.3×10^{-2} M, [Ph_2MeSiH] = 1.6×10^{-1} M, and [PPh_3] = 7.6×10^{-2}. (C) Relationship of [Ph_2MeSiH] and k_{obs} at [Ph_2MeSiH] = 1.4×10^{-1} to 4.9×10^{-1} M, [PPh_3] = 1.1×10^{-1} M, and [**1**] = 2.4×10^{-2} M.

Consequently, PPh_3 was added to the kinetic experiments to control the concentration of free phosphine. All kinetic experiments were conducted under anhydrous conditions using thoroughly dry reagents.

Concentration data were acquired by ^1H NMR spectroscopy by monitoring the disappearance of **2b** at −0.66 ppm (Re−OSi*Me*Ph_2) in the presence of phosphine and excess aldehyde. The concentration of siloxyrhenium hydride complex **2b** decayed exponentially during all reactions. Plots of ln[**2b**] vs time were linear, indicating that the reaction rate exhibits a pseudo-first-order dependence on [**2b**] (Figure 4A). The order of the reaction in aldehyde was determined by treating solutions of **2b** (1.56×10^{-2} M) and PPh_3 (7.21×10^{-2} M) with varying concentrations of *p*-anisaldehyde (5.8×10^{-2} M to 1.23 M). Plots of the k_{obs} values obtained in these experiments vs [*p*-anisaldehyde] reveal that the reaction rate exhibits a first-order dependence on the concentration of *p*-anisaldehyde (Figure 4B). However, as expected, at lower concentrations of *p*-anisaldehyde, the observed dependence of the reaction rate on the concentration of the substrate is no longer first order.

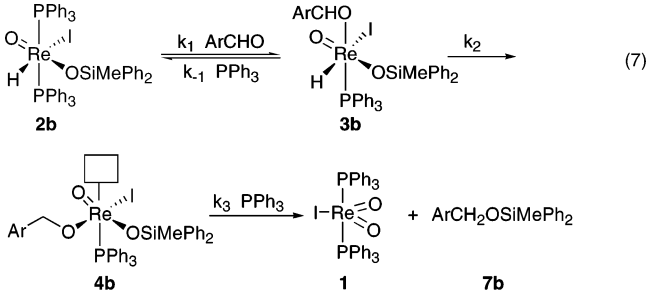

(7)

The kinetic order of the reaction (eq 6) in triphenylphosphine was determined next. As above, ^1H NMR spectroscopy was used to measure concentrations of reagents in solution. CD_2Cl_2 solutions of **2b** (1.87×10^{-2} M) and *p*-anisaldehyde (4.11×10^{-1} M) were treated with varying concentrations of PPh_3 (3.97×10^{-2} M to 1.54×10^{-1} M). Plotting $1/k_{obs}$ vs [PPh_3] for these experiments afforded a linear plot, demonstrating an inverse dependence of the reaction rate on the concentration of phosphine (Figure 5B). These data suggest that rapid and reversible phosphine dissociation precedes the rate-determining step of the stoichiometric hydrosilylation reaction (eq 7). A rate law for the stoichiometric hydrosilylation of *p*-anisaldehyde by **2b** that accounts for all the results above is presented in eq 8.

$$\text{rate} = \frac{k_1 k_2[\mathbf{2b}][p\text{-anisaldehyde}]}{k_{-1}[\text{PPh}_3] + k_2} = k_{obs}[\mathbf{2b}]$$

$$k_{obs} = \frac{k_1 k_2[p\text{-anisaldehyde}]}{k_{-1}[\text{PPh}_3] + k_2} \qquad (8)$$

The ratio of k_{-1}/k_2 as well as the value of k_1 was determined from the plot of $1/k_{obs}$ as a function of [PPh_3] (Figure 5B). The value of k_1 was calculated from the *y*-intercept, $1/(k_1[p\text{-anisaldehyde}])$,[26] and found to be 9.3×10^{-3} $M^{-1}\cdot s^{-1}$. From the slope, $k_{-1}/(k_1k_2[p\text{-anisaldehyde}])$,[26] and the above value of k_1, the ratio of k_{-1}/k_2 was determined to be 23.4 M^{-1}. The large value of this ratio supports the proposed rapid and reversible exchange of triphenylphosphine and *p*-anisaldehyde ligands prior to the rate-determining step.

(26) See Supporting Information for complete derivation.

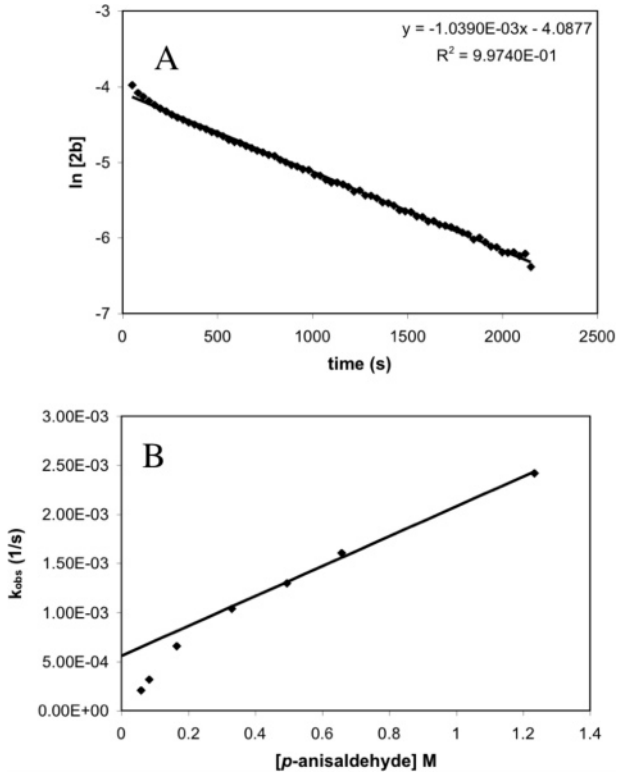

Figure 4. (A) A representative plot of the change in ln[**2b**] with time. The reaction was monitored by ^{1}H NMR spectroscopy for the disappearance of the Re−OSi*Me*Ph$_2$ signal at −0.66 ppm at 313 K: [**2b**] = 1.56 × 10^{-2} M, [PPh$_3$] = 7.21 × 10^{-2} M, [*p*-anisaldehyde] = 3.2 × 10^{-1} M. (B) Relationship between k_{obs} and [*p*-anisaldehyde] at the following concentrations: [**2b**] = 1.56 × 10^{-2} M, [PPh$_3$] = 7.21 × 10^{-2} M, [*p*-anisaldehyde] = 5.8 × 10^{-2} to 1.23 M.

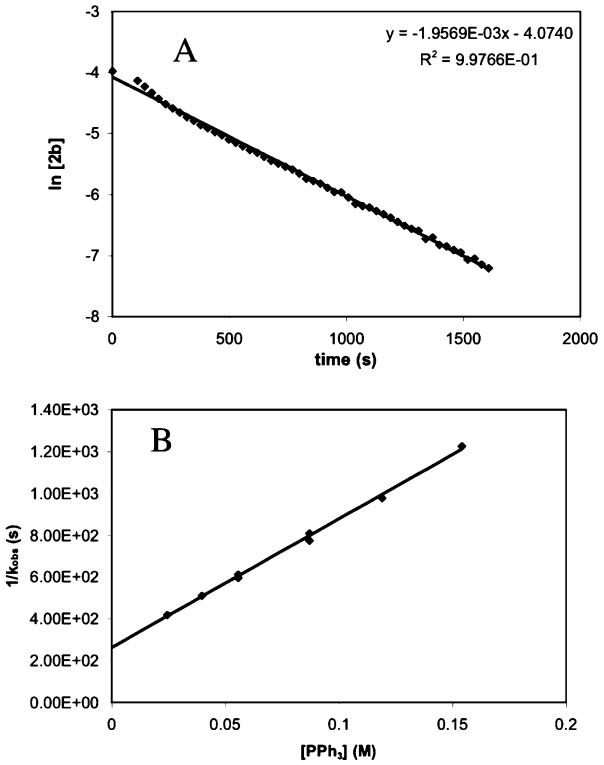

Figure 5. (A) Representative plot of the change of the ln[**2b**] with time. The reaction was monitored by ^{1}H NMR spectroscopy for the disappearance of the Re−OSi*Me*Ph$_2$ signal at −0.66 ppm at 313 K: [**2b**] = 1.87 × 10^{-2} M, [PPh$_3$] = 3.97 × 10^{-2} M, [*p*-anisaldehyde] = 4.11 × 10^{-1} M. (B) Relationship between $1/k_{obs}$ and [PPh$_3$] at the following concentrations: [**2b**] = 1.87 × 10^{-2} M, [*p*-anisaldehyde] = 4.11 × 10^{-1} M, [PPh$_3$] = 3.97 × 10^{-2} to 1.54 × 10^{-1} M ($1/k_{obs}$ = 6150[PPh$_3$] + 263).

Reversibility of Siloxyrhenium Hydride Formation. To test for reversibility in the formation of the siloxyrhenium hydride complexes **2**, complex **2b** (OSiPh$_2$Me) was treated with Me$_2$PhSiH under anhydrous conditions. The reaction was monitored by ^{1}H and ^{31}P{^{1}H} NMR spectroscopies; after 6 h at room temperature, no formation of **2a** was observed. Correspondingly, free Ph$_2$MeSiH was also not observed during the course of the reaction (eq 9). Treatment of **2a** with Ph$_2$MeSiH yielded similar

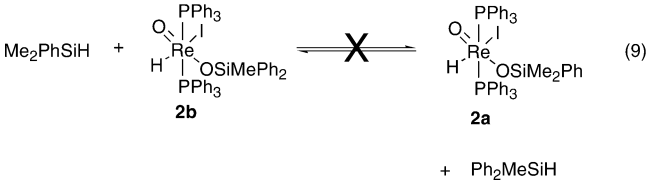

(9)

results after 5 h: (1) no formation of **2b** and (2) no generation of Me$_2$PhSiH. These results suggest that addition of silane across the Re−oxo bond is irreversible.

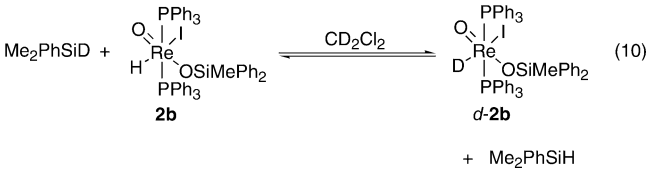

(10)

Hydride Exchange. Although the addition of silanes to **1** was found to be irreversible, the siloxyrhenium hydride complexes **2a** and **2b** were found to undergo H/D exchange with free silanes at room temperature. These reactions were observed by ^{1}H NMR when **2b** (0.022 mmol) was treated with Me$_2$PhSi−D (0.032 mmol, 1.5 equiv) under anhydrous conditions (eq 10).[27] After 30 min, the isotopic distribution of **2b** was determined to be 3.0:1.0 (**2b**/*d*-**2b**). The reaction reached an equilibrium isotopic distribution of 1.0:1.8 (**2b**/*d*-**2b**) after 6 h. We postulate that this H/D exchange reaction occurs by σ-bond metathesis after phosphine dissociation.[28]

Crossover Experiments. Crossover experiments were conducted under anhydrous conditions for the stoichiometric hydrosilylation of *p*-anisaldehyde. The reaction of *d*-**2a** and **2b** with *p*-anisaldehyde in CD$_2$Cl$_2$ at room temperature led to the formation of crossover products (eq 11). The exchange of siloxy

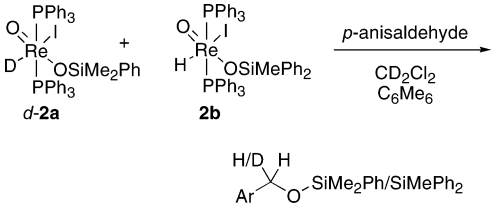

(11)

ligands was envisioned as a possible explanation for the results of the crossover experiment. Due to the overlapping chemical shifts of relevant resonances, however, direct observation of such

(27) No formation of Ph$_2$MeSiH or Ph$_2$MeSiD was observed.
(28) We cannot exclude the possibility that hydride exchange is occurring via oxidative addition, radical chain, or Lewis acid catalyzed processes.

a process by NMR was not feasible. Attempts to observe siloxy ligand exchange between **2a** and **2b** via triple labeling experiments were also unsuccessful.

To test for siloxy group exchange in **2a** and **2b**, efforts were focused on preparing an analogue of **2** with chemical shifts that could be distinguished from those of **2a** and **2b**. Previous reports have shown that alkoxyrhenium complexes undergo alkoxy ligand exchange with free alcohol, as well as with alkoxy groups.[29] Therefore, we envisioned the corresponding exchange of the siloxy ligand with free alcohol would provide synthetic access to novel alkoxyrhenium analogues of **2a** and **2b**. The exchange of a siloxy ligand for an alkoxy ligand to generate such complexes was extremely facile; treatment of **2b** with 10 equiv of methanol resulted in the formation the new alkoxyrhenium hydride complex **8** (eq 12). The ^{1}H NMR spectrum of **8**

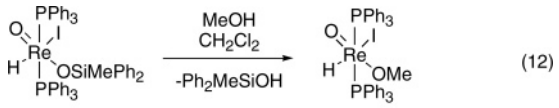

2b **8** (12)

is consistent with the formulation in eq 9; the rhenium-bound methoxy ligand is observed at δ 1.88 ppm (3H, s, Re−O*CH*$_3$), while the hydride ligand is observed at δ 4.91 ppm (t, 1H, Re−*H*). A single peak is observed at δ 11.0 ppm in the ^{31}P{^{1}H} NMR spectrum of **8**, indicating a *trans* arrangement of the phosphine ligands. Deep red X-ray quality crystals of **8** were obtained by layering pentane over a concentrated CH_2Cl_2 solution of **8**. The X-ray structure of **8** is presented in the Supporting Information. The rhenium center was found to possess octahedral geometry with the oxo ligand *trans* to the methoxide ligand. The hydride ligand was not located in the difference map, due to disorder in the iodide ligand, which exhibited partial (7.5%) occupancy of the hydride coordination site.

In order to obtain a non-disordered alkoxyrhenium hydride for analysis by X-ray diffraction, the analogous reaction of **2b** with 10 equiv of 4-methoxybenzyl alcohol was conducted, resulting in formation of complex **9** (eq 13). The ^{1}H [5.07 (t,

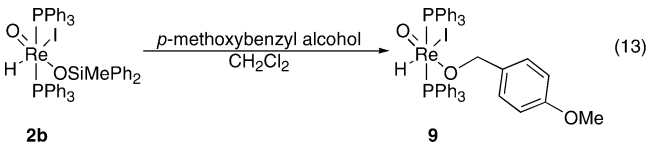

2b **9** (13)

1H, Re-*H*), 3.12 (2H, s, Re−O*CH*$_2$Ar)] and ^{31}P{^{1}H} [8.48] NMR data for this compound are consistent with the structure assigned to **9**. Orange-red, X-ray quality crystals were obtained by layering pentane over ether on top of a concentrated CH_2Cl_2 solution and cooling to −25 °C. An ORTEP diagram of the structure of **9** is presented in Figure 6, along with representative bond lengths and angles. Once again, the rhenium center was found to possess octahedral coordination geometry. The rhenium-bound hydride ligand, now observed in the difference map, was found to be oriented *trans* to the iodine

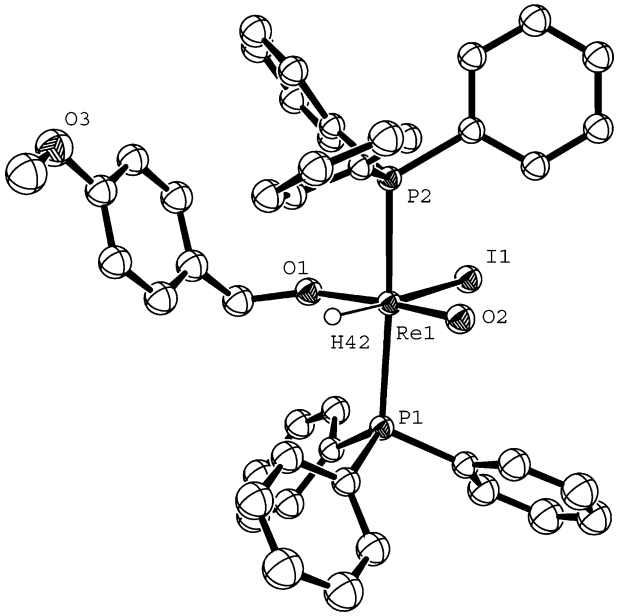

Figure 6. ORTEP drawing of **9**. H-atoms have been removed for clarity. Representative bond lengths (Å) and angles (deg): Re(1)−H(42), 1.680; Re(1)−O(1), 1.882; Re(1)−O(2), 1.705(6); Re(1)−P(1), 2.482(3); Re(1)−P(2), 2.483(3); P(1)−Re(1)−P(2), 173.9(6); O(1)−Re(1)−O(2), 173.7(0); Re(1)−O(2)−H(42), 91.7(7).

group as was previously proposed for **2b** and **8**.[30] The Re−O bond distance for the oxo group of **9** is slightly shorter than that in **2b** (1.705 Å) while the alkoxy Re−O bond is noticeably shorter (1.882 Å).

The ^{1}H NMR signal for the hydride ligand of the methoxyrhenium complex **8** is easily distinguished from that of siloxylrhenium hydride **2b**, thus providing the opportunity to probe for intermolecular siloxy/alkoxy ligand exchange by isotopic labeling experiments. The reaction of 1 equiv of *d*-**2b** with 1 equiv of **8** in CD_2Cl_2 was monitored by ^{1}H NMR spectroscopy under anhydrous conditions. Within 5 min, complex **2b** (undeuterated) was observed in the ^{1}H NMR spectrum. Correspondingly, the hydride ligand signal for **8** was observed to diminish (eq 14). These results suggest that the

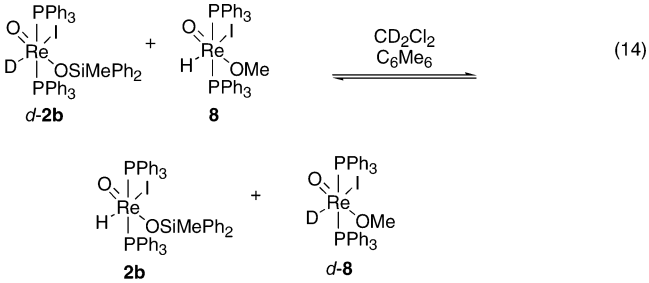

d-**2b** **8** **2b** *d*-**8** (14)

siloxy group of **2b** is labile and that a similar (albeit isotropic) ligand exchange reaction may occur during the course of catalytic hydrosilylation reactions involving **2**.[31]

Breakdown of Alkoxyrhenium Siloxy Intermediate. To gain more insight into the regeneration of **1** from **2** in the

(29) (a) Erikson, T. K. G.; Bryan, J. C.; Mayer, J. M. *Organometallics* **1988**, *7*, 1930. (b) Simpson, R. D.; Bergman, R. G. *Organometallics* **1993**, *12*, 781. (c) van Bommel, K. J. C.; Verboom, W.; Kooijman, H.; Spek, A. L.; Reddy, K. R. *Inorg. Chem.* **1998**, *37*, 4197.

(30) The Re−H bond length (1.68 Å) is notably shorter than those previously reported for oxorhenium hydrides: (a) For Re−H bond length in Tp*ReO(H)Cl = 1.69(8) Å, see Matano, Y.; Brown, S. N.; Northcutt, T. O.; Mayer, J. M. *Organometallics* **1998**, *17*, 2939. (b) Re−H bond length in Re(O)Cl_2(H)$(PPh_3)_2$ = 1.73(5) Å, see ref 9b.

(31) H/D exchange may be catalyzed by trace amounts of silane.

catalytic cycle, ^{18}O enriched benzaldehyde was treated with nonisotopically labeled siloxyrhenium hydride **2b**. To a solution of **2b** (0.19 mmol) in 1.20 mL of CH_2Cl_2, 0.61 mmol of $PhCH^{18}O$ (65% ^{18}O incorporation)[32] was added and the reaction mixture was stirred at room temperature under argon. After 3 h, the reaction mixture was analyzed by GC/MS, and the percentage of ^{18}O-enriched **7b** was determined to be 64.2 ± 0.1% (eq 15). This result clearly indicates that the oxygen of

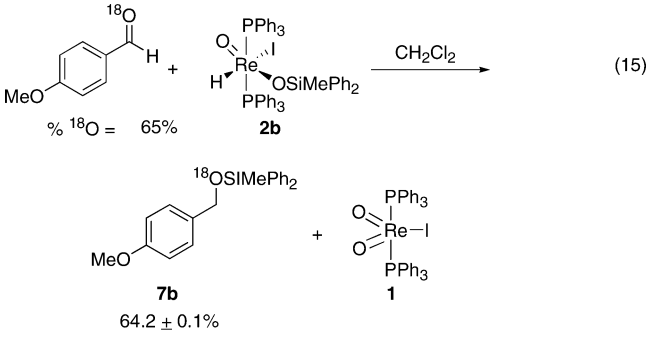

(15)

the benzaldehyde substrate is retained in the silyl ether product.

We propose that alkoxyrhenium siloxy intermediate **4** is formed by insertion of a datively bound carbonyl into the Re−H bond (eq 16). The collapse of putative intermediate **4** to form

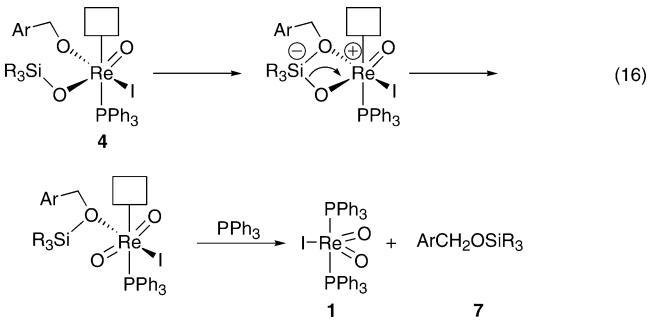

(16)

silyl ether **7** and dioxorhenium complex **1** may occur via a formal retro-[2 + 2] reaction. We envision this transformation beginning with silyl group transfer from the oxygen of the siloxy ligand to the oxygen of the alkoxy ligand. Literature reports of similar reactions suggest this may proceed via a five-coordinate silicon intermediate.[33] Ring opening of the strained silacycle would form the second oxo-ligand. We propose that liberation of the silyl ether and reassociation of triphenylphosphine subsequently generate **1**.

Reduction of an aldehyde by a siloxyrhenium hydride complex was also examined in the computational study by Lin, Wu, and co-workers. In their study, delivery of the hydride to the bound carbonyl was found to proceed through a lower energy transition state (18.4 kcal/mol) than that found for the siloxyrhenium hydride formation (37.7 kcal/mol). The siloxyrhenium alkoxy intermediate was found to be 4.4 kcal/mol more stable than the siloxyrhenium hydride complex. A second pathway for carbonyl reduction consisting of concerted delivery of the hydride and silyl groups to the carbonyl, similar to that described by Shvo and co-workers for their ruthenium hydride reduction of carbonyls,[34] was also evaluated by Lin, Wu, and co-workers. However, this pathway was found to be much higher in energy than the stepwise delivery of the hydride group. These results are consistent with our proposed formation of a siloxyrhenium alkoxy intermediate **4** from **3** by treatment of **2** with aldehyde.

Synopsis of Findings from Stoichiometric Reactions of 2a,b. Three complexes with the general formula of our proposed catalytic intermediate **2** were isolated and fully characterized. From these isolated complexes, several findings relevant to the mechanism by which the dioxorhenium complex **1** catalyzes hydrosilylation of carbonyl complexes were noted. These are as follows: (1) Siloxyrhenium hydride complexes **2** are formed by addition of silane across the Re−oxo bond without a requirement for phosphine dissociation. (2) Siloxyrhenium hydride complexes **2** are competent catalysts for the hydrosilylation of *p*-anisaldehyde with exogenous silane and perform these reactions with rates that are quantitatively identical to those obtained with **1**. (3) Siloxyrhenium hydride complexes **2** are effective reagents for the stoichiometric silyl and hydride transfer to *p*-anisaldehyde to form the hydrosilylation products in the absence of additional silane. (4) Kinetic studies on stoichiometric hydrosilylation of *p*-anisaldehyde with **2b** indicate that rapid, reversible phosphine dissociation occurs prior to a rate-determining aldehyde reduction step. (5) Siloxyrhenium hydride complexes **2** are substitutionally labile: they undergo facile H/D exchange and siloxy ligand exchange processes under nonanhydrous conditions. (6) Although the siloxy ligand of **2** is labile, overall addition of silane to **1** is irreversible under anhydrous conditions.

Catalytic Hydrosilylation Reactions. We next turned our attention to the working catalyst system, which, as illustrated in Scheme 1, begins with dioxorhenium complex **1**. Having studied the proposed intermediates **2a** and **2b** by stoichiometric experiments, we analyzed the *catalytic* hydrosilylation reactions involving the silanes corresponding to these complexes (Me_2PhSiH for **2a**, Ph_2MeSiH for **2b**).

At the onset of the hydrosilylation reaction of *p*-anisaldehyde with Me_2PhSiH catalyzed by **1**, a buildup of siloxyrhenium hydride complex **2a** was observed by ^1H NMR spectroscopy. Intermediate **2a** reached a maximum, steady concentration early in the reaction, and its concentration decreased near the end of the reaction. When the working catalyst system was monitored by $^{31}P\{^1H\}$ NMR, similar results were obtained: **2a** and a small quantity of free triphenylphosphine, as well as a trace amount of **1**, were observed during the course of the reaction.

The buildup of siloxyrhenium hydride complex **2a** in the working catalytic cycle was also observed by ESI-MS.[24,35] The hydrosilylation of *p*-anisaldehyde (7.7×10^{-2} M) with Me_2PhSiH (8.7×10^{-2} M) catalyzed by **1** (1.2×10^{-2} M) at room temperature was monitored by ESI-MS. At the start of the reaction, **1** was clearly observed at 743 *m*/*z* $[\mathbf{1} - I]^+$. However, 2 min after the addition of silane, complex **2a** was observed in the reaction mixture at 879 *m*/*z* $[\mathbf{2a} - I]^+$. After 20 min, complex **2a** was observed to be the predominant species present in solution.

Kinetic parameters were determined for the hydrosilylation of *p*-anisaldehyde with Me_2PhSiH catalyzed by **1**; these reactions

(32) Goering, H. L.; Dilgren, R. E. *J. Am. Chem. Soc.* **1960**, *82*, 5744.
(33) Chuit, C.; Corriu, R. J. P.; Reye, C.; Young, J. C. *Chem. Rev.* **1993**, *93*, 1371.
(34) Shvo, Y.; Czarkie, D.; Rahamim, Y. *J. Am. Chem. Soc.* **1986**, *108*, 7400.
(35) For reviews on the use of ESI-MS in the detection of catalytic intermediates, see: Plattner, D. A. *Int. J. Mass Spectrom.* **2001**, *207*, 125.

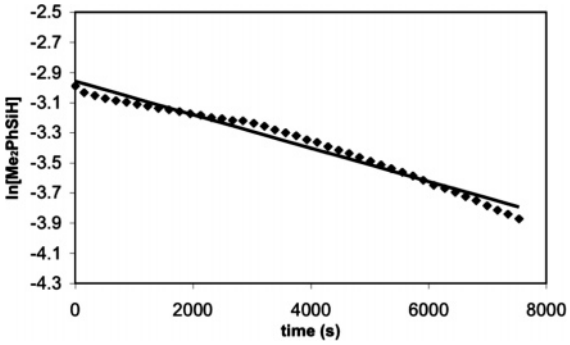

Figure 7. A representative plot of the change in ln[Me_2PhSiH] with time. The reaction was monitored by ^{1}H NMR spectroscopy for the disappearance of the *Me*$_2$PhSiH signal at 0.4 ppm at 313 K: [PPh_3] = 3.4×10^{-2} M, [*p*-anisaldehyde] = 1.8×10^{-1} M, [Me_2PhSiH] = 5.0×10^{-2} M, and [**1**] = 1.8×10^{-3} M ($R^2 = 0.974$; slope = -1.11×10^{-4}).

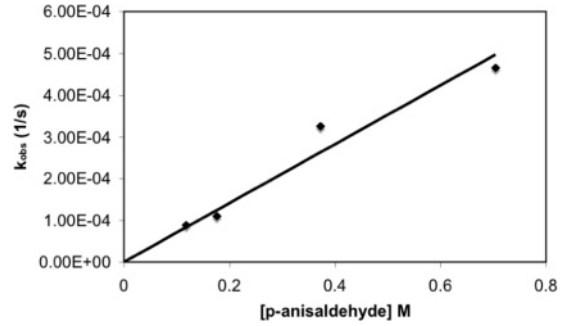

Figure 8. Relationship between k_{obs} and [*p*-anisaldehyde]. The reaction was monitored by ^{1}H NMR spectroscopy at 313 K in CD_2Cl_2 at the following concentrations: [Re] = 1.7×10^{-2} M, [Me_2PhSiH] = 5.0×10^{-2} M, and [PPh_3] = 3.0×10^{-2} M. [*p*-Anisaldehyde] was varied from 1.2×10^{-1} to 7.0×10^{-1}M ($R^2 = 0.947$; slope = 7.1×10^{-4} M^{-1} s^{-1}).

were carried out under anhydrous conditions with silane as the limiting reagent (eq 17).[36] Rate constants were determined from

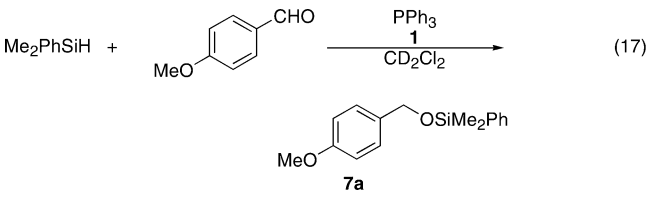

the disappearance of silane through 60−70% conversion. As described in the stoichiometric kinetic studies with **2a**, additional phosphine ligand was added to control the concentration of free phosphine in the reaction.

The relationship between ln[Me_2PhSiH] and time was linear, showing the reaction rate exhibits a first-order rate dependence on the concentration of silane (Figure 7). The linear plots of k_{obs} vs [*p*-anisaldehyde] (Figure 8) and k_{obs} vs [Re] (Figure 9) reveal that the reaction rate exhibits a first-order dependence on the concentration of the *p*-anisaldehyde, as well as on the concentration of rhenium. The rate of the catalytic reaction exhibits an inverse dependence on the concentration of PPh_3 as seen by examining the plot of $1/k_{obs}$ vs [PPh_3] (Figure 10).[37]

(36) All kinetics experiments for the catalytic reactions were carried out with excess aldehyde.

(37) The curvature of the plot of $1/k_{obs}$ vs [PPh_3] may suggest that the reaction rate exhibits a more complex dependence on the concentration of triphenylphosphine.

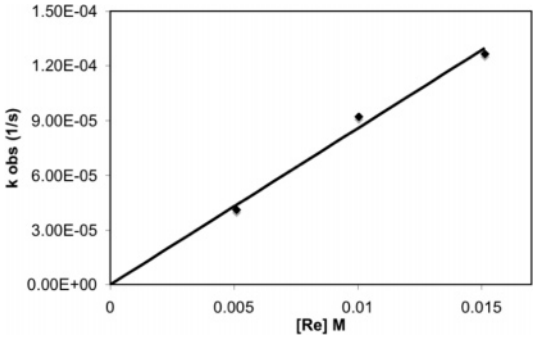

Figure 9. Relationship between k_{obs} and [Re] for the hydrosilylation of *p*-anisaldehyde with Me_2PhSiH catalyzed by **1**. The reaction was monitored by ^{1}H NMR spectroscopy at 313 K in CD_2Cl_2 at the following concentrations: [PPh_3] = 9.9×10^{-2} M, [*p*-anisaldehyde] = 5.9×10^{-1} M, and [Me_2PhSiH] = 8.0×10^{-2} M. The starting concentration of **1** was varied from 5.0×10^{-3} to 1.5×10^{-2} M ($R^2 = 0.985$; slope = 8.6×10^{-3} M^{-1} s^{-1}).

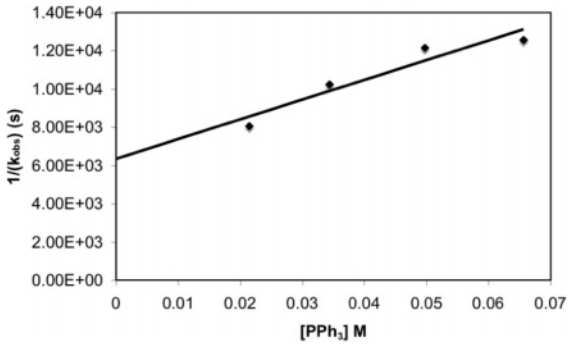

Figure 10. Relationship between $1/k_{obs}$ and [PPh_3]. The reaction was monitored by ^{1}H NMR spectroscopy at 313 K in CD_2Cl_2 at the following concentrations: [Re] = 3.6×10^{-3} M, [*p*-anisaldehyde] = 5.9×10^{-1} M, and [Me_2PhSiH] = 5.6×10^{-2} M. The concentration of PPh_3 was varied from 2.1×10^{-2} to 6.7×10^{-2} M ($R^2 = 0.91$; slope = 1.03×10^5 M^{-1} s^{-1}).

Scheme 3. Proposed Catalytic Cycle with Me_2PhSiH

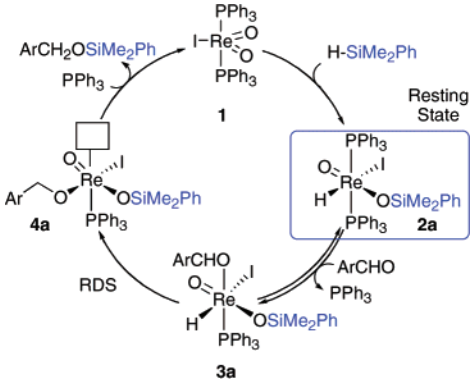

We conclude that complex **2a** is the resting state of the catalyst in the hydrosilylation of *p*-anisaldehyde with Me_2PhSiH (Scheme 3). Complex **2a** is observed to be the dominant species in the active catalytic reaction by ^{1}H and ^{31}P{^{1}H} NMR spectroscopy, as well as by ESI-MS. Analysis of the kinetics of the reaction suggests that formation of siloxyrhenium hydride complex **2a** is rapid. It also appears that a reversible ligand exchange occurs prior to rate-determining hydride transfer to the organic substrate.

Catalytic Hydrosilylation with Ph_2MeSiH. Kinetic parameters were determined for the hydrosilylation of *p*-anisaldehyde

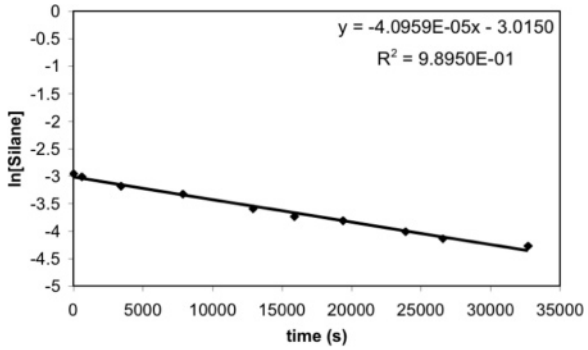

Figure 11. A representative plot of the change in ln[Ph_2MeSiH] with time. The reaction was monitored by ^1H NMR for the disappearance of the Ph_2MeSiH signal at 0.7 ppm at 313 K at the following concentrations: [PPh_3] = 1.6×10^{-1} M, [*p*-anisaldehyde] = 1.3×10^{-1} M, [Ph_2MeSiH] = 5.2×10^{-2} M, and [**1**] = 1.6×10^{-2} M.

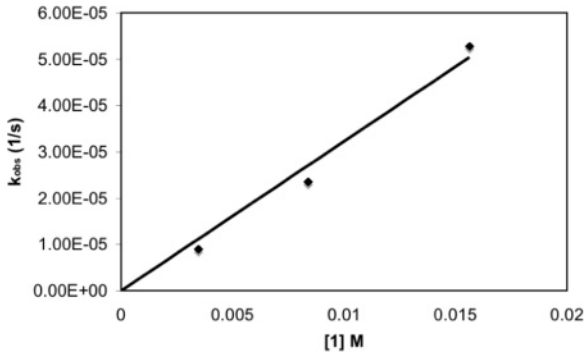

Figure 12. Relationship between k_{obs} and [**1**]. The reactions were conducted at the following concentrations: [PPh_3] = 2.0×10^{-1} M, [*p*-anisaldehyde] = 4.7×10^{-1} M, and [Ph_2MeSiH] = 5.2×10^{-2} M. The concentration of **1** was varied from 3.5×10^{-3} to 1.6×10^{-2} M (R^2 = 0.998; slope = 3.2×10^{-3} M^{-1} s^{-1}).

with Ph_2MeSiH catalyzed by **1** (eq 18). These studies suggestthe reaction with Ph_2MeSiH proceeds by the same mechanism as

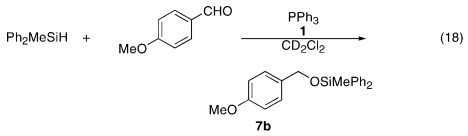

that observed with Me_2PhSiH but that, *under these reaction conditions*, the resting states of the two catalytic systems differ. The catalytic reactions with Ph_2MeSiH were monitored by ^1H NMR spectroscopy, and the concentration of Ph_2MeSiH displayed exponential decay. Plots of ln[Ph_2MeSiH] vs time were linear, indicating that the reaction kinetics exhibit first-order dependence on the concentration of silane (Figure 11). A plot of k_{obs} vs [**1**] was linear, indicating a first-order dependence of the reaction rate on the concentration of rhenium (Figure 12). Plots of k_{obs} vs [PPh_3] and k_{obs} vs [*p*-anisaldehyde] indicate no dependence of the reaction rate on the concentrations of free triphenylphosphine (Figure 13) or *p*-anisaldehyde (Figure 14). The reaction was also monitored by $^{31}P\{^1H\}$ NMR spectroscopy; these spectra showed only the presence of **1**. Similarly, the ^1H NMR spectrum did not reveal buildup of a detectable concentration of **2b** at any point in the reaction.[38]

From the kinetic data described above, we conclude that formation of **2b** is the rate determining step of the catalytic

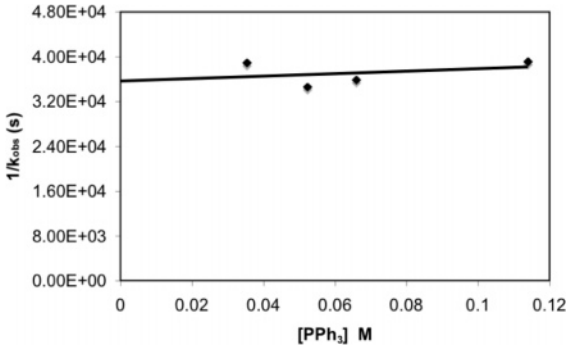

Figure 13. Relationship between $1/k_{obs}$ and [PPh_3]. The reaction was monitored by ^1H NMR spectroscopy at 313 K in CD_2Cl_2 at the following concentrations: [*p*-anisaldehyde] = 5.9×10^{-1} M, [**1**] = 8.3×10^{-3} M, and [Ph_2MeSiH] = 4.9×10^{-2} M. The concentration of PPh_3 was varied from 3.5×10^{-2} to 1.1×10^{-1} M.

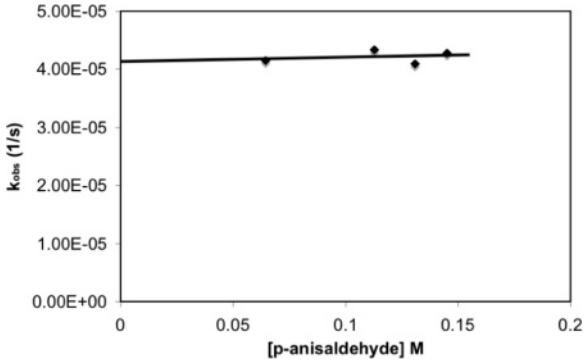

Figure 14. Relationship between k_{obs} and [*p*-aldehyde]. The reaction was monitored by ^1H NMR spectroscopy at 313 K in CD_2Cl_2 at the following concentrations: [PPh_3] = 1.6×10^{-1} M, [**1**] = 1.6×10^{-2} M, and [Ph_2MeSiH] = 5.2×10^{-2} M. The concentration of *p*-anisaldehyde was varied from 6.4×10^{-2} to 1.5×10^{-1} M.

Scheme 4. Proposed Catalytic Cycle with Ph_2MeSiH

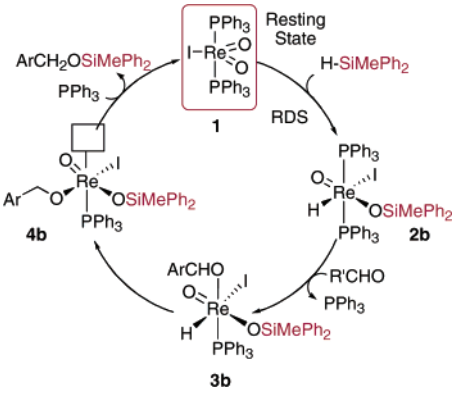

hydrosilylation of *p*-anisaldehyde by Ph_2MeSiH, revealing **1** as the resting state of the catalytic cycle in this case (Scheme 4). The only signal observed by $^{31}P\{^1H\}$ NMR during the catalytic reaction with Ph_2MeSiH is that of **1**. This result differs from our findings with Me_2PhSiH, supporting a change in relative rate constants for the two different systems. Our kinetic findings are supported by our observations of dominant catalytic species by $^{31}P\{^1H\}$ NMR for both systems (**2a** for Me_2PhSiH and **1** for Ph_2MeSiH).

Conclusion

$(PPh_3)_2(O)_2ReI$ has been shown to be a chemoselective catalyst for the hydrosilylation of carbonyl compounds, and the

(38) By adjusting the relative concentrations to allow for excess silane, the buildup of **2b** was observed.

mechanistic details have been elucidated. This reaction proceeds *via* an unprecedented mechanism that begins with the formation of a siloxyrhenium hydride complex **2**, which is stabilized by the presence of a spectator oxo ligand. The formation of **2** proceeds through a nondissociative mechanism, which begins with activation of the silane by the oxo ligand. This intermediate was isolated, identified crystallographically, and shown to be a competent catalyst for the reaction. The presence of **2** in the catalytic cycle is suggested by its ability to perform stoichiometric hydrosilylation of *p*-anisaldehyde in the absence of exogenous silane. Additionally, regeneration of **1** is observed by ^{1}H and ^{31}P{^{1}H} NMR and ESI-MS upon completion of the stoichiometric transfer of the hydride and silyl group from **2** to a carbonyl compound. Finally, isotopic labeling experiments support transfer of the silyl group from the siloxy ligand to the proposed alkoxy ligand resulting in retention of the aldehydic oxygen in the silyl ether product. In the catalytic hydrosilylation of *p*-anisaldehyde with Me_2PhSiH and **1**, **2a** is clearly observable spectroscopically. Kinetic analysis of this catalytic reaction suggests **2a** is the resting state of the catalytic cycle, indicating that reduction of the carbonyl compound is rate-determining. For catalytic hydrosilylation with Ph_2MeSiH, however, formation of the hydride was found to be the rate-determining step. In this case, **1** is observed to be the resting state of the catalytic cycle and **2b** is not observed. The ability of dioxorhenium catalyst **1** to catalyze the hydrosilylation of carbonyl compounds highlights a new mode of reactivity for high oxidation state metal complexes; with this mechanistic insight, new catalysts are being developed which will be reported in due course.

Experimental Section

General Procedures. Glassware was dried overnight at 150 °C prior to use. Infrared (IR) spectra were recorded using samples prepared as KBr pellets, and spectral data are reported in wavenumbers. NMR spectra were recorded with Bruker AV-300, AVB, AVQ-400, and DRX-500 spectrometers and referenced to residual peaks of CD_2Cl_2 unless otherwise noted. Mass spectrometric (MS) analyses were obtained at the University of California, Berkeley Mass Spectrometry Facility on VT ProSpec, ZAB2-EQ, and 70-FE mass spectrometers. Elemental analyses were performed at the University of California, Berkeley Microanalytical facility on a Perkin-Elmer 2400 Series II CHNO/S Analyzer. The crystal structures of **2b**, **8**, and **9** were solved by Drs. Fred Hollander and Allen Oliver at the UCB X-ray (CHEXRAY) facility.

Materials. Unless otherwise noted, reagents were purchased from commercial suppliers and used without further purification. Pentane, methylene chloride, and benzene were passed through columns of activated alumina (type A2, size 12 × 32) under nitrogen pressure and sparged with N_2 prior to use. Deuterated solvents were purchased from Cambridge Isotope Laboratories and purified by vacuum transfer from the appropriate drying agent (Na^0/Ph_2CO for C_6D_6, CaH_2 for CD_2Cl_2). **1**, **7a**, and **7b** were prepared as previously reported.[4] Anisaldehyde, dimethylphenylsilane, and diphenylmethylsilane were purchased from Aldrich and used as received for reactions performed on the benchtop. For reactions performed under inert atmosphere, these reagents were degassed by three freeze−pump−thaw cycles and then dried for 3 d over activated 3 Å molecular sieves. These reagents were filtered through a plug of neutral Al(III) under an inert atmosphere immediately before use. d_1-Dimethylphenysilane was prepared according to literature procedures.[39]

(39) Mori, A.; Fujita, A.; Kajiro, H.; Nishihara, Y.; Hiyama, T. *Tetrahedron* **1999**, *55*, 4573.

$(PPh_3)_2(O)(I)Re(H)OSi(CH_3)_2Ph$ (2a). In the glovebox,[40] $(PPh_3)_2Re(O)_2I$ (390 mg, 0.449 mmol) and dimethylphenylsilane (480 mg, 3.52 mmol) were combined in benzene (12 mL) in a scintillation vial equipped with a Teflon-coated stirbar. This heterogeneous dark purple/brown mixture was stirred briefly (∼30 s) and then allowed to stand at room temperature for 3 h. During this period, the mixture was stirred briefly several times (roughly once per hour) then allowed to settle. After this time, copious quantities of a pale green-gray precipitate had formed at the bottom of the vial. The dark brown benzene solution was decanted and set aside, leaving **2a** as a tan solid. The benzene solution was concentrated to a volume of roughly 7 mL and layered with pentane (3 mL). This resulted in the precipitation of a second crop of **2a**, which was combined with the first crop. The combined solids were washed with benzene (1 × 3 mL) then pentane (2 × 5 mL). Residual volatile materials were removed from **2a** *in vacuo*, leaving analytically pure powder (347 mg, 77%). Anal. Calcd for $C_{44}H_{42}IO_2P_2ReSi$: C, 52.54; H, 4.21. Found: C, 52.37; H, 4.54. IR (KBr, cm^{-1}): 1978 (ν_{Re-H}), 1094 ($\nu_{Re=O}$). ^{1}H NMR (400 MHz, CD_2Cl_2): δ 7.76 (d, 12H, J = 6.3 Hz), 7.35−7.45 (m, 18H), 7.29 (t, 1H, J = 7.2 Hz), 7.21 (t, 2H, J = 7.3 Hz), 7.11 (d, 2H, J = 7.0 Hz), 6.51 (t, 1H, J = 14.0 Hz), −0.75 (s, 6H). ^{13}C{^{1}H} NMR (CD_2Cl_2, 125 MHz): δ 140.1, 135.7 (t, J = 5.6 Hz), 133.9, 133.1 (t, J = 24.2 Hz), 131.9, 129.3, 128.9, 127.8, 0.45. ^{31}P{^{1}H} NMR (CD_2Cl_2, 162 MHz): δ 5.9 (s). ^{29}Si{^{1}H} NMR (CD_2Cl_2, 99 MHz): δ 7.5 (s). EI-MS (*m*/*z*): 879.1 [M − I]$^+$.

$(PPh_3)_2(O)(I)Re(D)OSi(CH_3)_2Ph$ (*d*-2a). For preparation of the deuterated compound, $(PPh_3)_2Re(O)_2I$ (420 mg, 0.483 mmol) was treated with d_1-dimethylphenylsilane (D−Si$(CH_3)_2$Ph, 691 mg, 5.03 mmol) in 10 mL of benzene. All other procedures were repeated as described for the synthesis of **2a**. Complex **2a**-*d* was isolated as a pale green-gray powder in one crop (301 mg, 62%). IR (KBr, cm^{-1}): 1451 (ν_{Re-D}), 1106 ($\nu_{Re=O}$). ^{1}H NMR (400 MHz, CD_2Cl_2): δ 7.74 (d, 12H, J = 6.3 Hz), 7.35−7.45 (m, 18H), 7.26 (t, 1H, J = 7.2 Hz), 7.11 (t, 2H, J = 7.3 Hz), 7.08 (d, 2H, J = 7.0 Hz), −0.77 (s, 6H). ^{2}H NMR (400 MHz, CD_2Cl_2): δ 6.55 (s). ^{13}C{^{1}H} NMR (CD_2Cl_2, 125 MHz): δ 135.7 (t, J = 7.0 Hz), 133.4, 132.5 (t, J = 30.5 Hz), 130.8, 128.7, 128.3, 127.3, −0.11. ^{31}P{^{1}H} NMR (CD_2Cl_2, 162 MHz): δ 5.9 (s). ^{29}Si{^{1}H} NMR (CD_2Cl_2, 99 MHz): δ 7.5 (s). EI-MS (*m*/*z*): 880.1 [M − I]$^+$.

$(PPh_3)_2(O)(I)Re(H)OSiPh_2CH_3$ (2b). For preparation of the diphenylmethylsiloxy compound, $(PPh_3)_2Re(O)_2I$ (468 mg, 0.539 mmol) was treated with diphenylmethylsilane (996 mg, 5.02 mmol) in 10 mL of benzene. All other procedures were repeated as described for the synthesis of **2a**. Complex **2b** was isolated as a pale gray powder (452 mg, 79%). Anal. Calcd for $C_{49}H_{44}IO_2P_2ReSi$: C, 55.10; H, 4.15. Found: C, 55.39 H, 4.13. IR (KBr, cm^{-1}): 2019 (ν_{Re-H}), 1093 ($\nu_{Re=O}$). ^{1}H NMR (400 MHz, CD_2Cl_2): δ 7.63 (d, 12H, J = 5.5 Hz), 7.26−7.41 (m, 20H), 7.15 (t, 4H, J = 7.5 Hz), 7.04 (d, 4H, J = 7.5 Hz), 6.49 (t, 1H, J = 14.0 Hz), −0.66 (s, 3H). ^{13}C{^{1}H} NMR (CD_2Cl_2, 125 MHz): δ 137.6, 135.6 (t, J = 5.0 Hz), 135.1, 132.9 (t, J = 23.8 Hz), 131.3, 129.5, 128.7, 127.8, 0.67. ^{31}P{^{1}H} NMR (CD_2Cl_2, 162 MHz): δ 4.5 (s). ^{29}Si{^{1}H} NMR (CD_2Cl_2, 99 MHz): δ −2.5 (s). EI-MS (*m*/*z*): 941.3 [M − I]$^+$.

$(PPh_3)_2(O)(I)Re(H)OCH_3$ (8). On the benchtop, methanol (70 μL, 1.73 mmol) was added to a solution of **2b** (166.5 mg, 1.56 mmol) in 4 mL of 1:1 benzene/CH_2Cl_2. The reaction was stirred overnight at rt. Solvent was removed *in vacuo*, and the resulting dark brown oil was diluted with 3 mL of benzene. To this solution were added ∼5 mL of pentane resulting in the formation of a brown/tan cloudy solution. This suspension was allowed to sit for ∼1 h. At this time, the solution had

(40) All the compounds described in this section (**2a**, *d*-**2a**, and **2b**) could alternatively be prepared on the benchtop without application of any air-sensitive handling techniques. However, compound yields from these benchtop preparations tended to be lower (50−60%) than yields for corresponding batches prepared in the glovebox. This discrepancy may be due to hydrolysis process; however, products **2a** and **2b** could be handled in air without deleterious effects.

turned transparent and **8** had crystallized out as brown crystals. The solvent was decanted off, and the crystals were washed with 1:1 ether/hexanes (3 × 4 mL) and then dried *in vacuo*. Anal. Calcd for $C_{37}H_{34}IO_2P_2Re$: C, 50.17; H, 3.87. Found: C, 50.20; H, 3.70. IR (KBr, cm^{-1}): 1991, 1095. ^1H NMR (500 MHz, CD_2Cl_2): δ 7.84−7.80 (m, 12H), 7.51−7.47 (m, 18H), 4.93 (t, 1H, J = 14.5 Hz), 1.90 (s, 3H). $^{13}C\{^1H\}$ NMR (CD_2Cl_2, 100 MHz): δ 134.8 (t, J = 5.0 Hz), 132.5 (t, J = 23.8 Hz), 130.7, 128.3 (t, J = 5.0 Hz), 58.8. $^{31}P\{^1H\}$ NMR (CD_2Cl_2, 162 MHz): δ 9.8.

$(PPh_3)_2$(O)(I)Re(H)OCH2Ph(*p*-OCH_3) (9). On the benchtop, *p*-methoxybenzyl alcohol (66 μL, 0.532 mmol) was added to a solution of **2b** (53.7 mg, 0.050 mmol) in 1.0 mL of CH_2Cl_2. The reaction was stirred overnight at rt. Solvent was removed *in vacuo*, and the resulting dark brown oil was diluted with 3 mL of benzene. To this solution was added ∼5 mL of pentane resulting in the formation of a brown/tan cloudy solution. This suspension was allowed to sit for ∼1 h. At this time, the solution had turned transparent and **9** had crystallized as dark reddish-brown crystals. The solvent was decanted off, and the crystals were washed with ether (3 × 4 mL) and then dried *in vacuo*. Anal. Calcd for $C_{44}H_{40}IO_3P_2Re$: C, 53.28; H, 4.06. Found: C, 53.61; H, 4.23. IR (KBr, cm^{-1}): 1995, 1095. ^1H NMR (500 MHz, CD_2Cl_2): δ 7.75−7.71 (m, 12H), 7.45−7.7.3 (m, 18H), 6.50 (d, 2H, J = 8.5 Hz), 6.03 (d, 2H, J = 8.5 Hz), 5.12 (t, 1H, J = 13.6 Hz), 3.73 (s, 3H), 3.12 (s, 2H). $^{13}C\{^1H\}$ NMR (CD_2Cl_2, 100 MHz): δ 158.6, 134.9 (t, J = 6 Hz), 132.4 (t, J = 24 Hz), 130.7, 128.8, 128.2 (t, J = 5 Hz), 73.0, 55.1. $^{31}P\{^1H\}$ NMR (CD_2Cl_2, 162 MHz): δ 9.7.

Acknowledgment. F.D.T. gratefully acknowledges the NIHGMS (R01 GM074774), the Camille and Henry Dreyfus Foundation, Research Corporation (Research Innovation Award), Merck Research Laboratories, Novartis, and Boehringer-Ingelheim for funding, and R.G.B. thanks the NSF (Grant CHE-0345488) for financial support

Supporting Information Available: Experimental procedures, sample spectra, and compound characterization data (PDF), and X-ray structure data (CIF). This material is available free of charge on the Internet at http://pubs.acs.org.

JA074477N